



# Normative Measurements of the Thyroid, Salivary Glands, and Tonsils on Imaging

Daniel Thomas Ginat

## 7.1 Thyroid Gland

- The thyroid gland is located in the visceral space of the neck and consists of two lobes connected by an isthmus anterior to the trachea.
- The thyroid gland has a high iodine content, resulting in high attenuation of 80–100 Hounsfield unit (HU) on non-contrast computed tomography (CT) and an attenuation of 150–170 HU on post-contrast CT (Fig. 7.1).
- The normal dimensions of the thyroid in adults are 40–60 mm in craniocaudal and 13–18 mm in anteroposterior dimensions (Fig. 7.2).
- The mean thyroid volume in adults is  $10.7 \pm 2.8$  mL (range: 5.7–17.1 mL) and the volume correlates with body size.
- The normal dimensions of thyroid gland in adult and pediatric groups are detailed in Tables 7.1 and 7.2.

---

D. T. Ginat (✉)

Department of Radiology, Section of Neuroradiology,  
University of Chicago, Chicago, IL, USA  
e-mail: [dtg1@uchicago.edu](mailto:dtg1@uchicago.edu)



**Fig. 7.1** Axial computed tomography (CT) images without (a) and with (b) contrast show the normally hyperattenuating and enhancing thyroid tissue



**Fig. 7.2** Normal thyroid gland. Ultrasound images and Tables 7.1 and 7.2 show the dimensions of the thyroid gland and its components

- The pyramidal lobe is a remnant of the thyroglossal duct and is a superior extension of normal thyroid tissue. Its presence is relevant for thyroid cancer surgery.
- The mean anteroposterior diameter, transverse diameter, and length of the pyramidal lobe are 2, 6, and 21 mm, respectively (Fig. 7.3).

**Table 7.1** Thyroid measurements in adults

Morphologic parameter	Size
Anteroposterior length, right (mm)	13.5 ± 2.0
Anteroposterior length, left (mm)	13.1 ± 1.8
Transverse length, right (mm)	16.0 ± 3.0
Transverse length, left (mm)	15.3 ± 2.5
Longitudinal length, right (mm)	42.5 ± 4.9
Longitudinal length, left (mm)	40.2 ± 3.8
Isthmus thickness (mm)	2.5 ± 1.0
Volume, right (cm <sup>3</sup> )	4.6 ± 2.0
Volume, left (cm <sup>3</sup> )	4.0 ± 1.4
Volume, total (cm <sup>3</sup> )	8.6 ± 3.1

**Table 7.2** Pediatric thyroid volumes by age

Age	Volume (cm <sup>3</sup> )
6	1.8 ± 0.4
8	1.8 ± 0.4
10	1.9 ± 0.5
12	2.8 ± 0.7
14	3.7 ± 0.7
16	5.0 ± 1.5

**Fig. 7.3** Pyramidal lobe. Axial computed tomography (CT) image shows the dimensions of the pyramidal lobe

### 7.1.1 Practical Implications

- Imaging can be obtained to evaluate patients with goiter and associated thyroid nodules, substernal extension, and tracheal narrowing (Fig. 7.4).
- When the longitudinal length of the lobes and the width of the whole gland together measure 6.5 cm or more, the thyroid gland can be considered enlarged.



**Fig. 7.4** Coronal computed tomography (CT) image shows goiter with tracheal narrowing

## 7.2 Parotid Gland and Ducts

- The parotid glands have a lobular morphology and can be divided into deep and superficial lobes, as well as an inferior projection referred to as the “tail,” which can be defined as the inferior 2 cm of the gland.
- Based on CT or magnetic resonance imaging (MRI), the maximum axial width can range from 26 to 69 mm; the depth can range from 33 to 86 mm; and the height can range from 38 to 80 mm (Fig. 7.5).

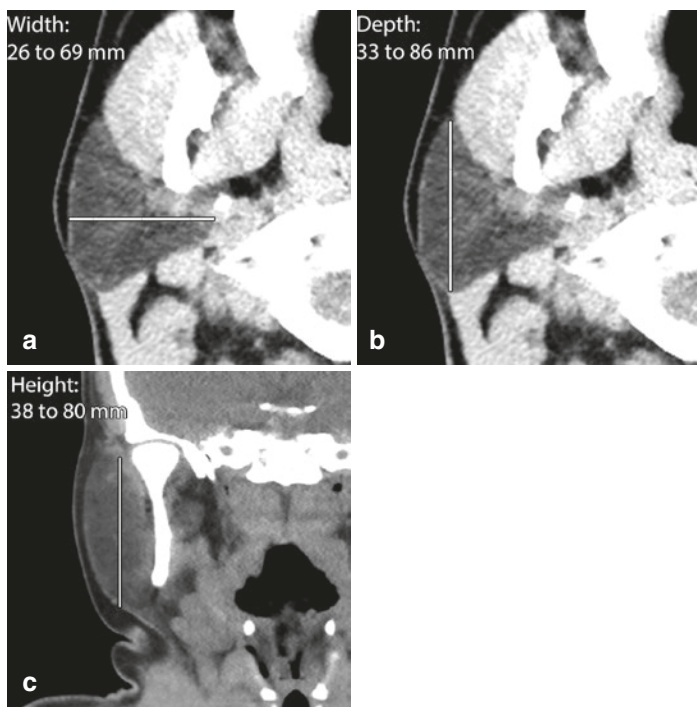


**Fig. 7.5** Axial (a and b) and coronal (c) computed tomography (CT) images with the range of normal dimensions of the parotid gland

- Based on ultrasound, the parotid glands measure  $46 \pm 8$  mm in the axis parallel to the mandibular ramus and  $37 \pm 6$  mm in a transverse axis.
- The volumes of parotid glands among different demographic groups are listed in Table 7.3.
- Besides the actual size of the parotid gland, it can be helpful to consider symmetry of the glands, in which the glands typically measure within 10% on either side.
- The attenuation of the parotid glands normally decreases with age as the gland undergoes fatty infiltration (Fig. 7.6).

**Table 7.3** Normal parotid gland volume

Demographic group	Volume (cm <sup>3</sup> )
Adolescent males	17–21
Adolescent females	14–17
Young adult males	20–24
Young adult females	18–21
Middle-aged males	29–35
Middle-aged females	20–22
Elderly males	29–35
Elderly females	29–35

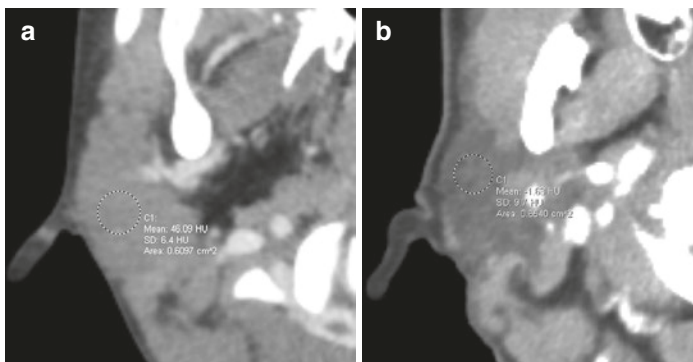


**Fig. 7.6** Axial computed tomography (CT) images show higher attenuation of the parotid gland in a child (a) than in an adult (b)

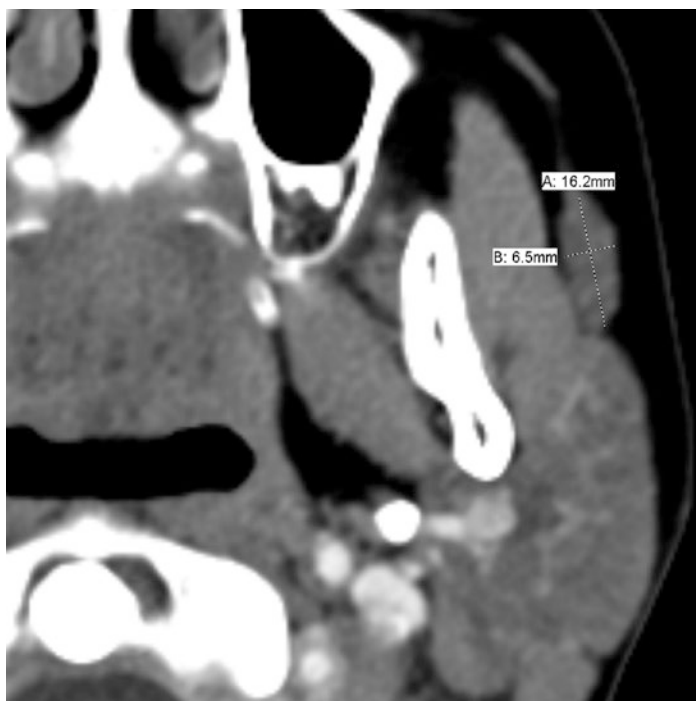


**Fig. 7.7** Axial computed tomography (CT) image shows an accessory parotid gland

- The mean size of the accessory parotid gland is 16 mm × 6 mm and the mean distance from the main parotid gland is 10 mm (Fig. 7.7).
- The mean parotid duct length is 50 mm.
- The mean width of the parotid duct is normally 1–2 mm (Fig. 7.8).

### 7.2.1 Practical Implications

- Enlargement of the parotid gland can be due to sialosis, infectious and inflammatory sialadenitis, and neoplasm

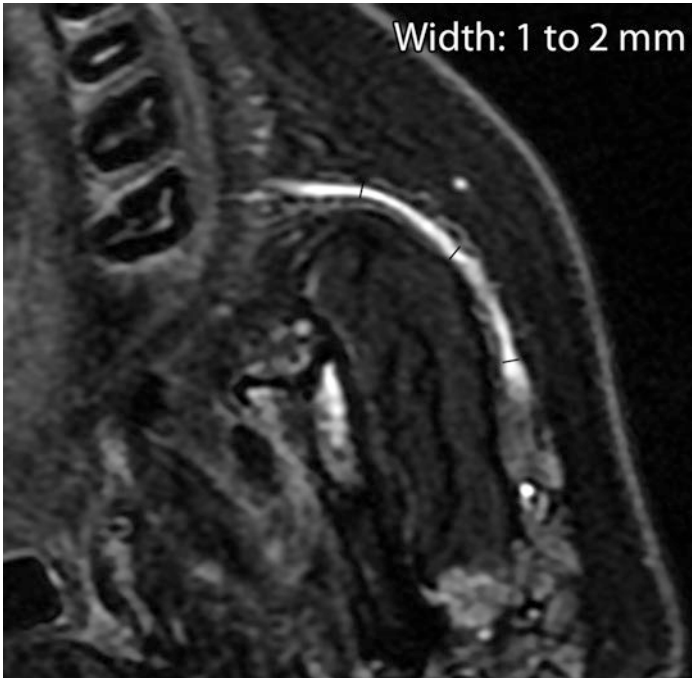


**Fig. 7.8** Axial T2-weighted magnetic resonance imaging (MRI) shows a normal fluid-filled parotid duct

(Fig. 7.9). Some of these conditions can also be associated with parotid ductal dilatation (Fig. 7.10).

- A small parotid gland can result from post-inflammatory atrophy or can appear reduced in size after partial parotidectomy (Fig. 7.11).

---

### 7.3 Submandibular Gland and Ducts

- The normal submandibular gland measures  $28 \times 18$  mm ( $\pm 5$  mm) in the axial plane (Fig. 7.12).
- The volume of submandibular glands in different demographic groups are listed in Table 7.4.

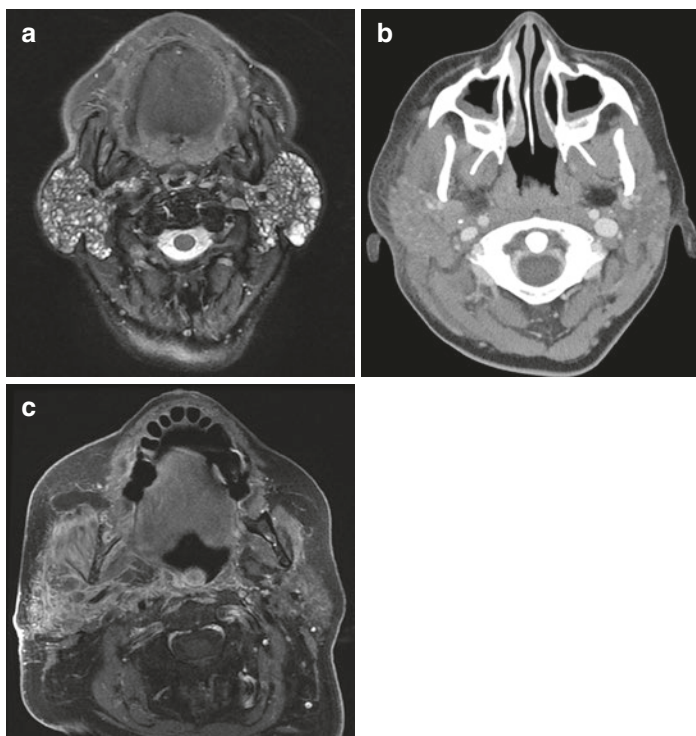


**Fig. 7.9** Axial T2-weighted magnetic resonance imaging (MRI) shows enlarged parotid glands with multiple cysts related to Sjogren syndrome (a). Axial computed tomography (CT) image shows right parotid swelling related to parotitis with surrounding inflammation (b). Axial fat-suppressed post-contrast T1-weighted MRI shows diffuse infiltration of the right parotid gland from carcinoma (c)

- The mean length of the submandibular duct is 58 mm and the submandibular duct genu has a mean angle of  $115^{\circ}$  (Fig. 7.13).
- The mean width of the submandibular duct is 2–3 mm.
- An intra- or extra-glandular duct diameter of 3 mm or more indicates possible obstruction.



**Fig. 7.10** Parotid ductal enlargement. Axial T2-weighted MRI shows dilatation of the bilateral parotid ducts, left greater than right, due to post-inflammatory strictures

### 7.3.1 Practical Implications

As with the parotid glands, the submandibular glands can be enlarged due to sialadenitis or neoplasm (Fig. 7.14). On the other hand, the glands can be small after radiation therapy or chronic inflammation (Fig. 7.15). Enlargement of the submandibular duct can be congenital due to an imperforate submandibular duct, or result from obstruction by tumors, post-inflammatory strictures, and calculi (Fig. 7.16).

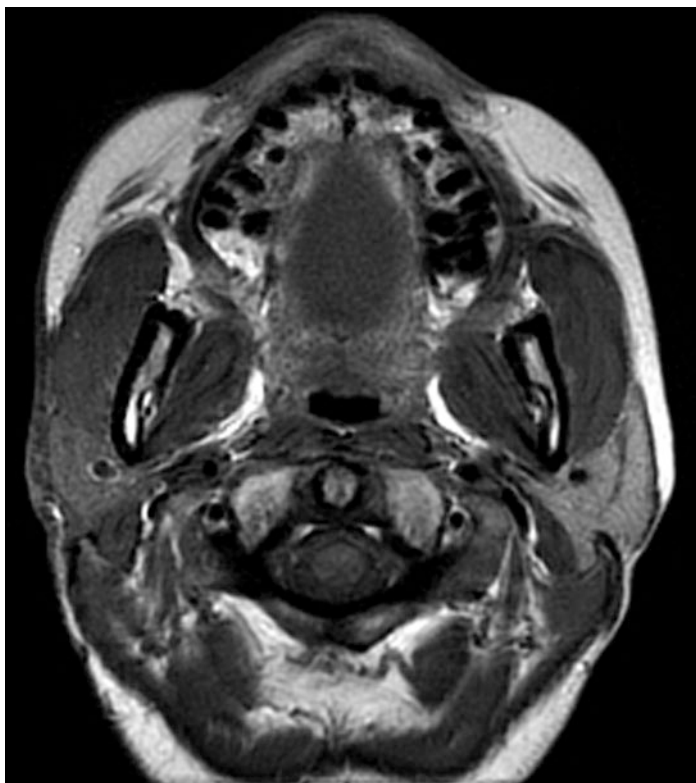


**Fig. 7.11** Axial T1-weighted magnetic resonance imaging (MRI) shows a small amount of residual right parotid tissue following parotidectomy with scar tissue in the overlying subcutaneous tissues

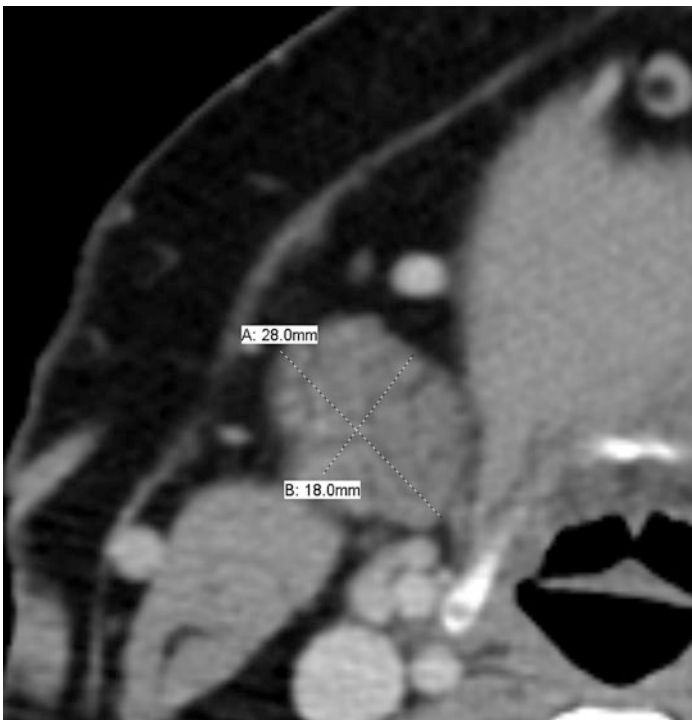
---

## 7.4 Tonsils

- The tonsils comprise the lingual, palatine, and nasopharyngeal (adenoid) tonsils.
- The tonsils grow proportionally to the skeletal structures during childhood.

**Table 7.4** Normal submandibular gland volume

Demographic group	Volume (cm <sup>3</sup> )
Adolescent males	7.2–8.9
Adolescent females	6.5–8.1
Young adult males	7.8–9.5
Young adult females	7.3–8.6
Middle-aged males	8.4–10.2
Middle-aged females	7.9–9.3
Elderly males	8.3–10.5
Elderly females	7.0–8.2

**Fig. 7.12** Axial computed tomography (CT) image shows a normal submandibular gland

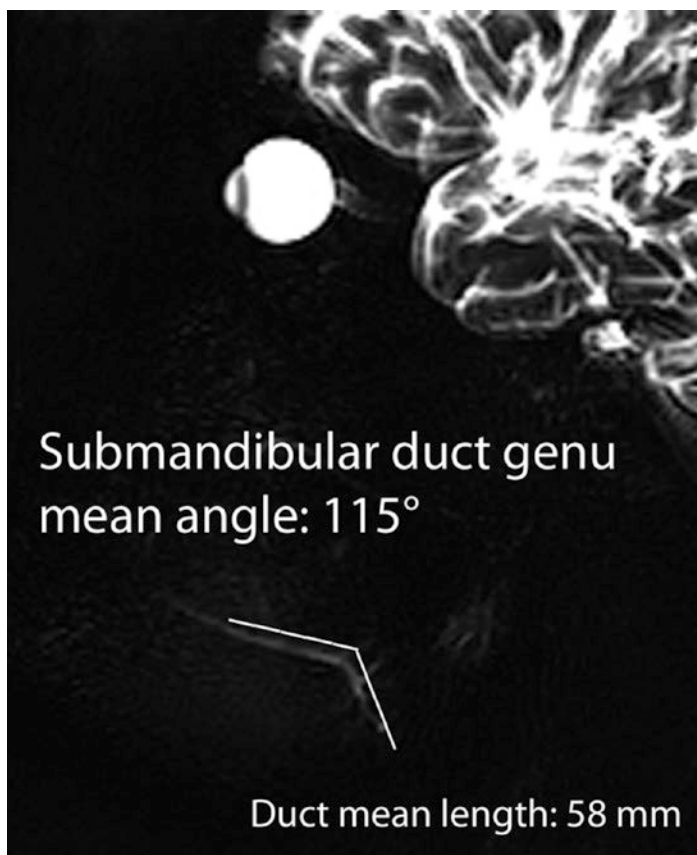


**Fig. 7.13** Submandibular duct. Sagittal oblique magnetic resonance (MR) sialogram image shows the normal dimension of a normal submandibular duct

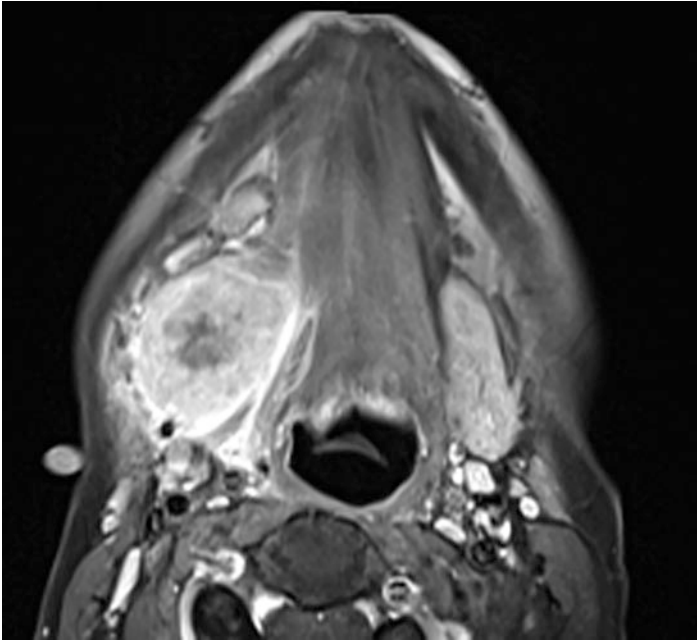


**Fig. 7.14** Axial post-contrast T1-weighted MRI shows enlargement of the right submandibular gland due to an infiltrating carcinoma

- The adenoids are largest in the 7–10 years age group with a mean of 15 mm and steadily decline to 5 mm by 60 years of age (Fig. 7.17).
- The lingual tonsils typically measure less than 10 mm in thickness (Fig. 7.18).
- The normal adult palatine tonsils measure up to 12 mm × 20 mm in axial section (Fig. 7.19).

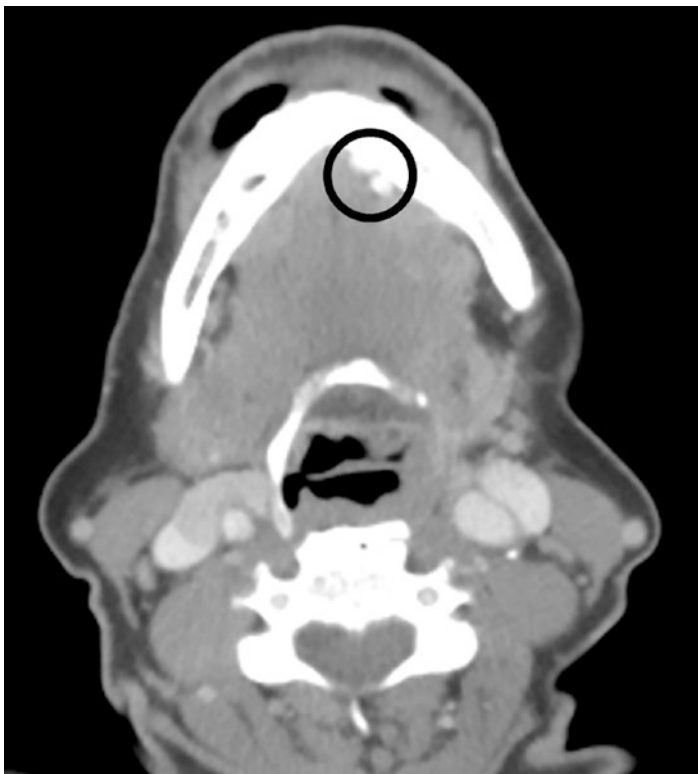


**Fig. 7.15** Axial CT image shows atrophy of the left submandibular gland due to chronic sialadenitis from calculi (encircled)

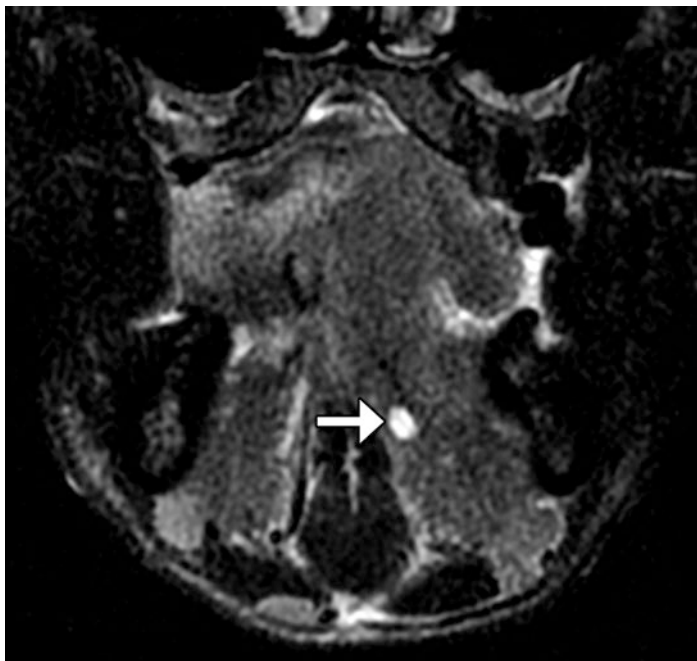


**Fig. 7.16** Submandibular duct dilatation. Coronal T2-weighted magnetic resonance imaging (MRI) shows a dilated left submandibular duct (arrow) due to obstruction by tumor

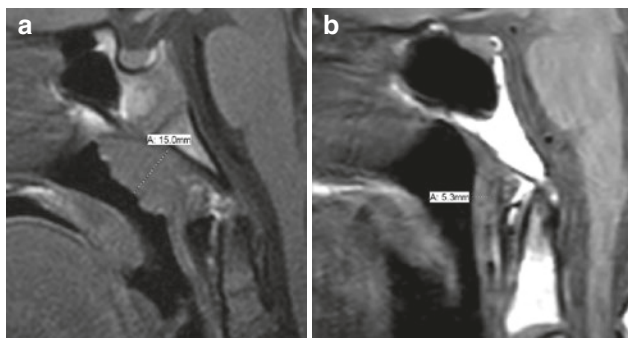


**Fig. 7.17** Sagittal T1-weighted MR images in a child (a) and adult (b) show normal adenoids



**Fig. 7.18** Sagittal post-contrast T1-weighted magnetic resonance imaging (MRI) shows the normal lingual tonsils

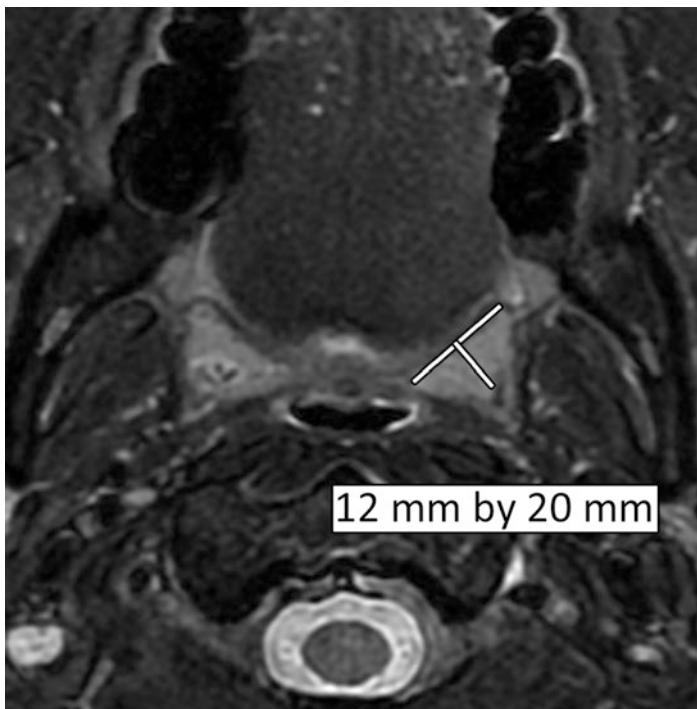


**Fig. 7.19** Axial fat-suppressed T2-weighted magnetic resonance imaging (MRI) shows normal palatine tonsils

#### **7.4.1 Practical Implications**

The tonsillar tissues can be enlarged due to benign lymphoid hyperplasia, infection, or neoplasm (Fig. 7.20).

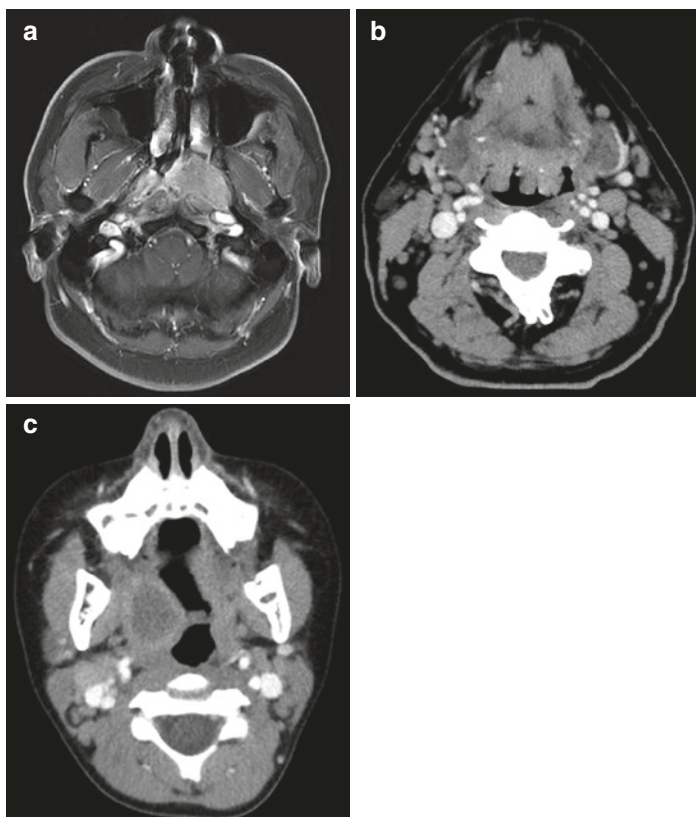


**Fig. 7.20** Axial post-contrast T1-weighted magnetic resonance imaging (MRI) shows a nasopharyngeal carcinoma (a). Axial computed tomography (CT) image shows lingual tonsil hyperplasia (b). Axial CT image shows right tonsillitis with peritonsillar abscess (c)

## Further Reading

- Aasen S, Kolbenstvedt A. CT appearances of normal and obstructed submandibular duct. *Acta Radiol.* 1992;33(5):414–9.
- Ahn D, Yeo CK, Han SY, Kim JK. The accessory parotid gland and facial process of the parotid gland on computed tomography. *PLoS One.* 2017;12(9):e0184633.
- Atkinson C, Fuller J 3rd, Huang B. Cross-sectional imaging techniques and normal anatomy of the salivary glands. *Neuroimaging Clin N Am.* 2018;28(2):137–58.
- Bhatia KS, King AD, Vlantis AC, Ahuja AT, Tse GM. Nasopharyngeal mucosa and adenoids: appearance at MR imaging. *Radiology.* 2012;263(2):437–43.
- Ceylan I, Yener S, Bayraktar F, Secil M. Roles of ultrasound and power Doppler ultrasound for diagnosis of Hashimoto thyroiditis in anti-thyroid marker-positive euthyroid subjects. *Quant Imaging Med Surg.* 2014;4(4):232–8.
- Dost P. Ultrasonographic biometry in normal salivary glands. *Eur Arch Otorhinolaryngol.* 1997;254(Suppl 1):S18–9.
- Dost P, Kaiser S. Ultrasonographic biometry in salivary glands. *Ultrasound Med Biol.* 1997;23(9):1299–303.
- Fricke BL, Donnelly LF, Shott SR, Kalra M, Poe SA, Chini BA, Amin RS. Comparison of lingual tonsil size as depicted on MR imaging between children with obstructive sleep apnea despite previous tonsillectomy and adenoidectomy and normal controls. *Pediatr Radiol.* 2006;36(6):518–23.
- Friedman M, Wilson MN, Pulver TM, et al. Measurements of adult lingual tonsil tissue in health and disease. *Otolaryngol Head Neck Surg.* 2010;142(4):520–5.
- Ginat DT. Imaging of benign neoplastic and nonneoplastic salivary gland tumors. *Neuroimaging Clin N Am.* 2018;28(2):159–69.
- Hamilton BE, Salzman KL, Wiggins RH, Harnsberger HR. Earring lesions of the parotid tail. *AJNR Am J Neuroradiol.* 2003;24(9):1757–64.
- Hong HS, Lee JY, Jeong SH. Normative values for tonsils in pediatric populations based on ultrasonography. *J Ultrasound Med.* 2018;37(7):1657–63.
- Horsburgh A, Massoud TF. The salivary ducts of Wharton and Stenson: analysis of normal variant sialographic morphometry and a historical review. *Ann Anat.* 2013;195(3):238–42.
- Ivanac G, Rozman B, Skreb F, Brkljacić B, Pavić L. Ultrasonographic measurement of the thyroid volume. *Coll Antropol.* 2004;28(1):287–91.
- Kim DW, Jung SL, Baek JH, Kim J, Ryu JH, Na DG, Park SW, Kim JH, Sung JY, Lee Y, Rho MH. The prevalence and features of thyroid pyramidal lobe, accessory thyroid, and ectopic thyroid as assessed by computed tomography: a multicenter study. *Thyroid.* 2013;23(1):84–91.

- Larsson SG, Lufkin RB, Hoover LA. Computed tomography of the submandibular salivary glands. *Acta Radiol.* 1987;28(6):693–6.
- Li W, Sun ZP, Liu XJ, Yu GY. [Volume measurements of human parotid and submandibular glands]. *Beijing Da Xue Xue Bao Yi Xue Ban.* 2014;46(2):288–93.
- Mahne A, El-Haddad G, Alavi A, et al. Assessment of age-related morphological and functional changes of selected structures of the head and neck by computed tomography, magnetic resonance imaging, and positron emission tomography. *Semin Nucl Med.* 2007;37(2):88–102.
- Medbery R, Yousem DM, Needham MF, Kligerman MM. Variation in parotid gland size, configuration, and anatomic relations. *Radiother Oncol.* 2000;54(1):87–9.
- Prince JS, Stark P. Normal cross-sectional dimensions of the thyroid gland on routine chest CT scans. *J Comput Assist Tomogr.* 2002;26(3):346–8.
- Raz E, Saba L, Hagiwara M, Hygino de Cruz LC Jr, Som PM, Fatterpekar GM. Parotid gland atrophy in patients with chronic trigeminal nerve denervation. *AJNR Am J Neuroradiol.* 2013;34(4):860–3.
- Vogler RC, Ii FJ, Pilgram TK. Age-specific size of the normal adenoid pad on magnetic resonance imaging. *Clin Otolaryngol Allied Sci.* 2000;25(5):392–5.